Variational Quantum Solutions for the Hubbard Dimer

Benchmark Analysis: Exact Diagonalization, Lattice DFT, and VQE

Kauê Miziara

2026-02-03

Table of contents

1. Introduction

1.1 Project Overview

This project implements a multi-method computational study of the Hubbard Dimer, a fundamental model in condensed matter physics. The primary objective is to evaluate the efficacy of classical and quantum-classical hybrid algorithms in capturing electronic correlation.

By defining a framework-agnostic pipeline, this work benchmarks three distinct approaches:

1. **Full Configuration Interaction (FCI):** Direct numerical diagonalization.
2. **Lattice Density Functional Theory (LDFT):** Classical mean-field approximation.
3. **Variational Quantum Eigensolver (VQE):** Quantum-native optimization using the Hardware-Efficient Ansatz (HEA).

1.2 The Importance of Condensed Matter Physics

Condensed matter physics explores the macroscopic and microscopic properties of matter, especially in phases where interactions between many particles are strong. Understanding these interactions is the bottleneck for developing high-temperature superconductors, efficient catalysts, and novel semiconductor materials.

> The central challenge in the field is the **Many-Body Problem**. Since electrons are indistinguishable fermions, their wavefunctions are anti-symmetric and highly entangled.

In "strongly correlated" systems, the behavior of a single electron cannot be described independently of the others, rendering single-particle approximations (like basic *Hartree-Fock* or standard *DFT*) physically insufficient.

1.3 Objectives

The *Hubbard Dimer* is the simplest non-trivial realization of the *Hubbard model*. It is used here as a controlled environment to study the **Mott Transition**.

This project serves as an exercise to:

- Validate the manual implementation of **Jordan-Wigner transformations**.
- Quantify the **Correlation Energy Gap** where classical Lattice DFT deviates from exact solutions.
- Demonstrate the successful recovery of this correlation energy using **Variational Quantum Algorithms**.

2. Physical Foundations

2.1 The Many-Body Problem and Computational Complexity

The central challenge in quantum chemistry and condensed matter physics is the Many-Body Problem. For a system of N interacting electrons, the wavefunction $\Psi(\mathbf{r}_1, \mathbf{r}_2, \dots, \mathbf{r}_N)$ depends on $3N$ spatial coordinates and N spin coordinates.

Since electrons are fermions, the wavefunction must be anti-symmetric under the exchange of any two particles, leading to complex correlation effects.

2.1.1 The Exponential Wall

The Hilbert space dimension of a quantum system scales exponentially with the number of particles. For a system with M orbitals and N electrons, the number of possible configurations (basis states) is given by the binomial coefficient:

$$\dim(\mathcal{H}) = \binom{2M}{N}$$

This exponential scaling renders *Exact Diagonalization* (FCI) computationally intractable for systems exceeding a few dozen electrons. Classical approximations are required to map this many-body complexity onto simpler, tractable models.

2.2 The Hubbard Model

The Hubbard model is the simplest approximation used to study the transition between **conducting** and **insulating** phases in solid-state systems.

It simplifies the full electronic structure by assuming electrons only occupy discrete *lattice sites* and only interact when they reside *on the same* site.

2.2.1 The Hubbard Hamiltonian

In quantum mechanics, the Hamiltonian (H) is the operator corresponding to the total energy of the system. For the Hubbard model, the Hamiltonian is expressed as:

$$H = -t \sum_{\langle i,j \rangle, \sigma} (c_{i\sigma}^\dagger c_{j\sigma} + c_{j\sigma}^\dagger c_{i\sigma}) + U \sum_i n_{i\uparrow} n_{i\downarrow}$$

In which:

- $c_{i\sigma}^\dagger, c_{i\sigma}$: Creation and annihilation operators for an electron at site i with spin σ.
- $n_{i\sigma}$: Number operator ($n_{i\sigma} = c_{i\sigma}^\dagger c_{i\sigma}$).
- σ: Spin index, typically $\uparrow$ (up) or $\downarrow$ (down).
- t: Hopping integral (kinetic energy scale).

- U: On-site Coulomb repulsion (potential energy scale).

† The Hopping Term (Kinetic Energy)

The term $-t(c_{i\sigma}^{\dagger}c_{j\sigma} + c_{j\sigma}^{\dagger}c_{i\sigma})$ describes the kinetic behavior of the system:

- **Annihilation ($c_{j\sigma}$):** Removes an electron from site j.
- **Creation ($c_{i\sigma}^{\dagger}$):** Places an electron at site i.

The sum of these operations represents the tunneling of an electron between adjacent sites. This process lowers the kinetic energy of the system by allowing electrons to delocalize across the lattice.

† The Interaction Term (Potential Energy)

The term $U(n_{i\uparrow}n_{i\downarrow})$ describes the electronic correlation:

- **Number Operators ($n_{i\uparrow}, n_{i\downarrow}$):** These operators return the occupancy of the specific spin state at site i, which could be either 0 or 1.
- **On-site Repulsion:** The product $n_{i\uparrow}n_{i\downarrow}$ is non-zero only when site i is doubly occupied. In this case, the system's energy is increased by U, representing the electrostatic repulsion between two electrons in the same spatial orbital.

2.2.2 Fock Space and Second Quantization

To represent states with varying numbers of particles, we utilize **Fock Space** ($\mathcal{F}$), which is the direct sum of Hilbert spaces for $N = 0, 1, 2, ...$ particles.

A state in this space is represented by an occupation number vector:

$$|\psi\rangle = |n_1, n_2, ..., n_M\rangle$$

where $n_i \in \{0, 1\}$ represents the occupancy of the i-th spin-orbital.

† Creation and Annihilation Operators

The dynamics in Fock space are governed by operators that transition between these occupancy states:

1. **Creation Operator ($c_i^{\dagger}$):** Places an electron in orbital i.

$$c_i^{\dagger} |n_1, ..., 0_i, ..., n_M\rangle = (-1)^{\sum_{k<i} n_k} |n_1, ..., 1_i, ..., n_M\rangle$$

2. **Annihilation Operator (c_i):** Removes an electron from orbital i.

$$c_i |n_1, ..., 1_i, ..., n_M\rangle = (-1)^{\sum_{k<i} n_k} |n_1, ..., 0_i, ..., n_M\rangle$$

The phase factor $(-1)^{\sum_{k<i} n_k}$ tracks the number of occupied states preceding the i-th site, ensuring that the operators satisfy the **canonical anti-commutation relations**:

$$\{c_i, c_j^{\dagger}\} = \delta_{ij}$$

$$\{c_i, c_j\} = \{c_i^{\dagger}, c_j^{\dagger}\} = 0$$

2.3 The Jordan-Wigner Mapping

The fundamental difficulty in quantum simulation is that qubit operators (Pauli gates) commute when acting on different qubits ($[X_i, X_j] = 0$), whereas fermion operators must anti-commute ($\{c_i, c_j\} = 0$).

The Jordan-Wigner mapping solves this by representing the fermion operators as a combination of Pauli matrices and a "parity string" of Z operators:

$$c_j^\dagger \to \left(\bigotimes_{k<j} Z_k\right) \otimes \sigma_j^+ \otimes \left(\bigotimes_{j<k<N} \mathbb{I}_k\right)$$

$$c_j \to \left(\bigotimes_{k<j} Z_k\right) \otimes \sigma_j^- \otimes \left(\bigotimes_{j<k<N} \mathbb{I}_k\right)$$

2.3.1 Interpretation of the Mapping

- **The Raising/Lowering Operators:** The term $\sigma^\pm$ corresponds to the qubit ladder operators $\sigma_\pm$, which flip the state of the j-th qubit between $|0\rangle$ and $|1\rangle$. It is such as:

$$\sigma^\pm = \frac{1}{2}(X \mp iY)$$

$$(\sigma^+)^\dagger = \sigma^- \leftrightarrow (\sigma^-)^\dagger = \sigma^+$$

- **The Parity String:** The string of Z operators ($Z_0 \otimes Z_1 \otimes \cdots \otimes Z_{j-1}$) stores the cumulative parity of the preceding qubits. This ensures that when an operation is performed on site j, the resulting state picks up the correct physical sign (-1) required by the Pauli Exclusion Principle.

2.4 The Mott Transition and Double Occupancy

The Mott transition is a metal-to-insulator transition driven by electron-electron correlations rather than traditional band theory.

In a standard metal, electrons are delocalized and can flow freely under an electric field. However, in certain materials, the repulsive force between electrons becomes so strong that they "lock" into position, one per site, effectively halting conduction.

2.4.1 The Competition of Scales

The state of the system is determined by the ratio U/t:

- **Weakly Correlated Regime ($U/t \ll 1$):** Kinetic energy dominates. Electrons delocalize across the lattice to minimize their energy, and the system behaves as a metal.
- **Strongly Correlated Regime ($U/t \gg 1$):** Potential energy dominates. The cost of two electrons occupying the same site (U) outweighs the energy gain from hopping (t). The electrons localize to avoid the penalty, leading to a **Mott Insulator**.

2.4.2 Double Occupancy as a Physical Observable

To quantify this transition, we define the **Double Occupancy** ($\langle D \rangle$), which measures the average number of sites containing two electrons:

$$\langle D \rangle = \frac{1}{L} \sum_{i=1}^{L} \langle n_{i\uparrow} n_{i\downarrow} \rangle$$

Where L is the number of sites.

In the non-interacting limit ($U = 0$), electrons are distributed statistically, and $\langle D \rangle$ is at its maximum. As U increases, $\langle D \rangle$ serves as an order parameter for the Mott transition; its decay toward zero is the signature of electrons localizing and the system entering the insulating phase.

2.5 The Hubbard Dimer

The Hubbard Dimer is the $L = 2$ case of the model, representing two sites with four possible spin-orbitals: $0\uparrow, 0\downarrow, 1\uparrow, 1\downarrow$. At **half-filling** ($N = 2$ electrons), it is the smallest system that captures the physics described above.

In the dimer, the Mott transition is manifested as the crossover between:

1. **The Bonding Singlet State:** For $U = 0$, the ground state is a superposition where both electrons share the lower-energy spatial orbital.
2. **The Localized (Heisenberg) Limit:** For $U \to \infty$, the ground state approaches a configuration where each site is occupied by exactly one electron with opposite spins, minimizing U while maintaining the lowest possible symmetry-allowed energy.

2.6 The Limitations of Exact Solvers

While *Full Configuration Interaction* (FCI), which is the direct diagonalization of the Hamiltonian, provides the exact ground state energy and wavefunction, its application is severely limited by the dimensionality of the problem.

2.6.1 Basis State Explosion

As previously established, the Hilbert space dimension grows binomially with the number of orbitals. For a Hubbard model with L sites at half-filling ($N = L$), and considering spin degrees of freedom ($2L$ spin-orbitals), the size of the Hamiltonian matrix is:

$$\dim(\mathcal{H}) = \binom{2L}{L}$$

For $L = 2$ (Dimer), the dimension is $\binom{4}{2} = 6$, trivial for modern hardware. However, for a system of only $L = 20$ sites, the dimension exceeds 137 billion.

Storing such a matrix in memory requires hundreds of gigabytes, and diagonalizing it to find the lowest eigenvalue becomes computationally prohibitive.

2.6.2 The Need for Approximations

Since most industrially relevant materials and chemical catalysts involve hundreds (or thousands) of electrons, we cannot rely on exact methods.

Common techniques employed are:

1. **Classical Mean-Field Theories (DFT):** These reduce the many-body problem to a single-particle problem by approximating the complex electron-electron interactions.
2. **Variational Quantum Algorithms (VQE):** These leverage quantum hardware to represent the exponentially large wavefunction in a naturally compressed format, using the variational principle to find the ground state.

2.7 Lattice Density Functional Theory (LDFT)

Density Functional Theory (DFT) is the most widely used classical method for electronic structure calculations.

It is based on the Hohenberg-Kohn theorems, which state that the ground state properties of a many-electron system are uniquely determined by its electron density profile rather than its complex many-body wavefunction.

2.7.1 The Kohn-Sham Approach

To make the problem tractable, the interacting many-body system is mapped onto a system of non-interacting particles moving in an effective local potential.

In the context of the Lattice Hubbard model, this effective potential must account for the on-site repulsion U without explicitly calculating the two-body correlations.

2.7.2 The Hartree Potential and Mean-Field Approximation

The primary approximation used in this project is the **Mean-Field (Hartree) approximation**.

We replace the two-body interaction term $Un_{i\uparrow}n_{i\downarrow}$ with a single-particle potential where each electron interacts with the *average* density of electrons with opposite spin:

$$V_{i,\sigma}^{Hartree} = U\langle n_{i,-\sigma}\rangle$$

This transforms the complex interaction term into a site-dependent potential energy.

The Hamiltonian becomes "linearized" in terms of single-particle operators, which can be solved using standard matrix diagonalization.

2.7.3 The Self-Consistent Field (SCF) Loop

Since the Hartree potential depends on the electron densities ($\langle n\rangle$), and the densities are determined by the eigenvectors of the Hamiltonian, the problem must be solved iteratively.

This is known as the **Self-Consistent Field (SCF) loop**:

1. **Initialization:** Assume an initial guess for the site densities $\langle n_{i\sigma}\rangle$.
2. **Construct Hamiltonian:** Build the effective single-particle Hamiltonian using the current densities to calculate the Hartree potential.
3. **Diagonalization:** Solve the Hamiltonian to find the new single-particle wavefunctions (Kohn-Sham orbitals).
4. **Density Update:** Calculate the new densities from the occupied orbitals.
5. **Convergence Check:** Compare the new densities with the previous iteration. If the change is below a defined threshold, the system is "Self-Consistent"; otherwise, repeat from step 2.

2.7.4 The Correlation Gap

While LDFT is computationally efficient, its reliance on the average density means it fails to capture **dynamical correlation**.

In the high-U regime of the Hubbard Dimer, the mean-field approximation significantly underestimates the energy because it cannot properly account for the "instantaneous" avoidance between electrons.

This discrepancy between the DFT result and the Exact solution is known as the **Correlation Energy**.

2.8 The Variational Quantum Eigensolver (VQE)

The *Variational Quantum Eigensolver* is a hybrid quantum-classical algorithm designed to find the ground state energy of a given Hamiltonian.

While DFT relies on approximating the interaction potential, VQE utilizes the **Variational Principle** to optimize a trial wavefunction (Ansatz) until it approximates the true many-body ground state.

2.8.1 The Variational Principle

The mathematical foundation of VQE is the variational theorem, which states that, for any normalized trial wavefunction $|\psi(\theta)\rangle$, the expectation value of the Hamiltonian H is always an upper bound to the true ground state energy E_0:

$$E(\theta) = \frac{\langle\psi(\theta)|\, H\, |\psi(\theta)\rangle}{\langle\psi(\theta)|\psi(\theta)|\psi(\theta)|\psi(\theta)\rangle} \geq E_0$$

The goal of the algorithm is to minimize $E(\theta)$ by iteratively adjusting the parameters θ using a classical optimizer.

2.8.2 Hybrid Quantum-Classical Workflow

The VQE distributes the computational load between quantum and classical hardware:

1. **Quantum Processor (QPU):** Prepares the state $|\psi(\theta)\rangle$ on a quantum register and measures the expectation values of the Pauli strings that compose the Hamiltonian.
2. **Classical Processor (CPU):** Sums the measured expectation values to calculate the total energy $E(\theta)$ and uses an optimization algorithm (e.g., Adam, COBYLA) to suggest new parameters θ.

2.8.3 Overcoming the Correlation Gap

Unlike the mean-field approach of DFT, which reduces electron interactions to an average potential, the VQE prepares a state on the QPU that can naturally represent entanglement and complex correlations.

By using a sufficiently expressive **Ansatz**, the VQE can explore the full Hilbert space and converge to the exact FCI energy, effectively recovering the correlation energy that classical approximations lose in the high-U regime.

2.9 Linking Theory and Computation

The mathematical complexity of the Jordan-Wigner transformation and the iterative nature of the SCF and VQE loops necessitate an architecture that prioritizes modularity and numerical precision.

The following section details the software engineering principles employed to translate these physical foundations into a scalable, framework-agnostic codebase.

3. Software Architecture

3.1 Design Philosophy: Separation of Concerns

The project is built on the principle of **Separation of Concerns (SoC)**. By decoupling the physical definitions (Hamiltonians, Models) from the mathematical backends (Numpy, PennyLane), the library ensures that the physics remains immutable regardless of the computational tool used.

This is achieved through several key engineering patterns:

- **Abstraction Layer:** The algebra is handled by an abstract base class, ensuring the same physical logic can be executed on a classical CPU or a Quantum Simulator/Processor.
- **Modularity:** Physics modules (Hubbard Model, Jordan-Wigner mapping) are independent of the solver logic (DFT, VQE).
- **Extensibility:** The architecture is designed to support additional backends (e.g., Qiskit) without requiring changes to the core physics engine.

3.2 Framework-Agnostic Algebra

At the core of the system is the `OperatorBackend` interface. This abstract layer defines the standard operations required for many-body physics, such as:

- Matrix multiplication and inner products.
- Diagonalization (Eigenvalue problems).
- Tensor products (Kronecker products) for building multi-site operators.
- Pauli string manipulation for quantum circuits.

3.2.1 Dependency Injection

The solvers (both `LatticeDFT` and `VQESolver`) do not instantiate their own backends. Instead, they use **Dependency Injection**.

A concrete backend (e.g., `NumpyBackend`) is passed to the solver at runtime. This allows for:

1. **Unit Testing:** Replacing complex backends with mocks for faster testing.
2. **Framework Swapping:** Running the same Hubbard Model instance through a classical exact solver and then a quantum VQE solver by simply injecting a different backend.

3.3 Project Structure

The repository is organized to reflect these architectural layers:

- `src/`: The core library.
  - `algebra/`: Contains the `OperatorBackend` interface and concrete implementations (e.g. `Numpy`, `PennyLane`).

  - `physics/`: Defines the Hubbard Model, creation/annihilation operators, and the Jordan-Wigner Mapper.
  - `quantum/`: Houses the VQE infrastructure, including Ansätze (HEA, HVA) and the optimization loops.
  - `visualization/`: Decoupled plotting utilities for benchmarking results across phases.
- `scripts/`: Executable code with implementation-specific workflows for benchmarking (Phase 1 through 4).

3.4 Development Stack and Tooling

The project utilizes a standardized Python toolchain focused on static analysis, type safety, and automated quality control.

3.4.1 Package and Environment Management

- **`uv`:** Employed as the primary package manager and build system. It provides high-performance dependency resolution and manages the virtual environment, ensuring reproducible builds across development environments.

3.4.2 Static Analysis and Code Quality

- **Ruff:** Used for linting and code formatting. It enforces a consistent style guide and identifies potential logic errors or dead code.
- **Pyright:** Acts as the static type checker. By enforcing strict type hinting across the library, it prevents runtime type errors and typing inconsistencies.

3.4.3 Automation and Testing

- **pytest:** The testing framework used to validate physical constants, operator anti-commutation relations, and solver convergence. The test suite is designed for modularity, allowing individual components (e.g., the Jordan-Wigner Mapper) to be verified independently.
- **pre-commit:** Manages Git hooks to execute Ruff, Pyright and Pytest checks automatically before every commit, ensuring that only code meeting the quality baseline enters the repository.

4. Methodology

4.1 Phase 1: Algebraic Foundations and Fermionic Mapping

4.1.1 Objectives

The primary goal of Phase 1 was to build the fundamental operator algebra required for the Hubbard model.

This involved establishing the computational basis for a multi-site system and implementing the transformation logic to represent fermionic operators in a matrix format.

4.1.2 Physical Implementation: The Jordan-Wigner Mapper

The core technical challenge was translating the second-quantization operators ($c_i, c_i^\dagger$) into a concrete numerical representation while preserving the Pauli Exclusion Principle.

The `JordanWignerMapper` was implemented to systematically construct multi-qubit operators. For a system with N spin-orbitals, the mapper builds the parity strings (Z chains) required to maintain anti-commutation. This was verified by testing the fundamental relation $\{c_i, c_j^\dagger\} = \delta_{ij}$ across the generated matrices.

4.1.3 Software Architecture: The First Concrete Backend

To execute these operations, the first iteration of the base `OperatorBackend` class was implemented:

- **NumpyBackend:** Utilizes `numpy` for dense matrix representations and linear algebra operations.
- **Kronecker Products:** Multi-site operators were built using recursive tensor products to scale the 1-body and 2-body operators to the full 2^N Hilbert space.

4.1.4 Results

Phase 1 was concluded with a verified library of basic operators:

- **Creation/Annihilation matrices** for arbitrary site counts.
- **Number Operators** ($\hat{n}_i$) for each spin-orbital.
- **Total Number Operator** ($\hat{N}_{total} = \sum \hat{n}_i$).

The successful implementation of these operators provided the necessary building blocks for the implementing the complete Hubbard Hamiltonian in Phase 2.

4.2 Phase 2: Exact Solution and Symmetry Sector Enforcement

4.2.1 Objectives

The goal of Phase 2 was to establish a "Ground Truth" for the Hubbard Dimer by performing **Full Configuration Interaction** (FCI).

This involved constructing the Hamiltonian (integrating both hopping and interaction terms) and diagonalizing the resulting matrix to observe the physical transition from a metallic to an insulating state.

4.2.2 The Electron Ejection Problem

During initial executions, the exact solver yielded unphysical results in the high-U regime.

Since it was built without constraints (which was wrong), the numerical diagonalization prioritized the global minimum of the 4-qubit Hilbert space.

As U increased, the energy cost of maintaining two electrons on a 2-site lattice ($N = 2$) eventually exceeded the energy of states with fewer electrons. Consequently, the solver "ejected" an electron to avoid the U penalty, settling in the $N = 1$ sector.

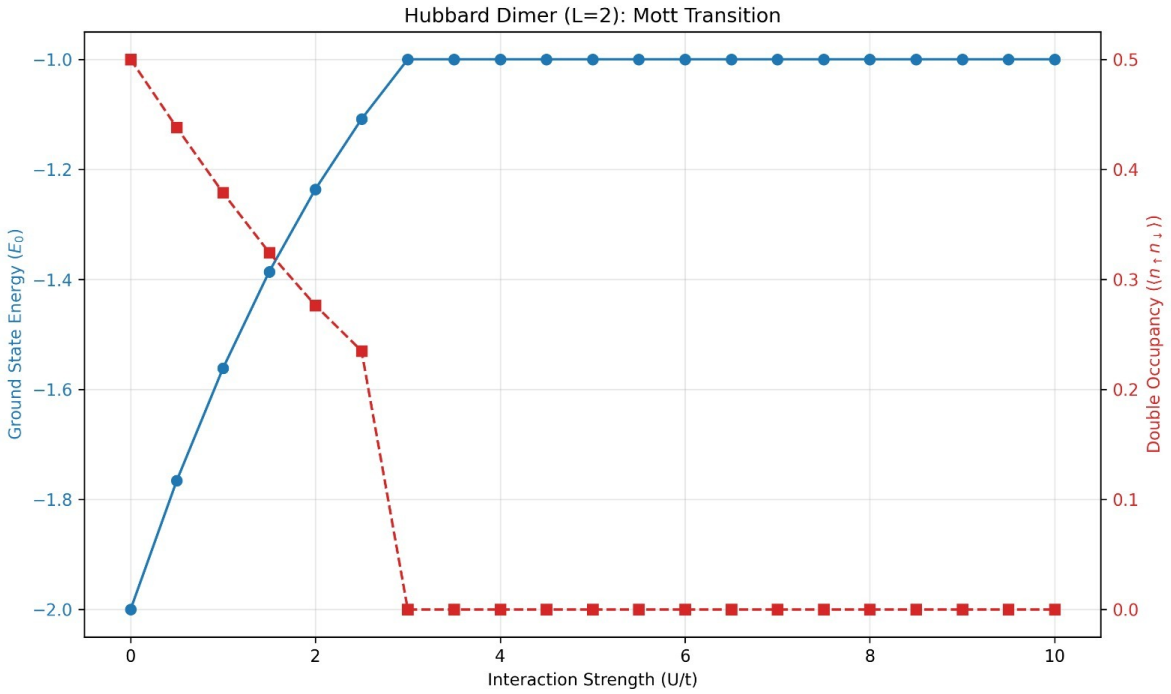

Figure 1: Hubbard Dimer (L=2): Electron Ejection

This resulted in an energy plateau at approximately -1.0 and a sudden drop in double occupancy to zero, effectively failing to represent the Mott physics of a closed system.

4.2.3 Fix: Particle Number Projection

To fix this, the solver logic was updated to enforce the **half-filling regime** (forcing $N = 2$). This was implemented by:

1. Diagonalizing the full Hamiltonian to obtain the set of all eigenvalues and eigenvectors.
2. Projecting each eigenvector onto the **Total Number Operator** ($\hat{N}$) built in Phase 1.
3. Filtering the results to select only the lowest energy state satisfying $\langle\psi|\,\hat{N}\,|\psi\rangle = 2$.

4.2.4 Results and Physics Analysis

With the $N = 2$ constraint applied, the system correctly demonstrated the **Mott Transition**:

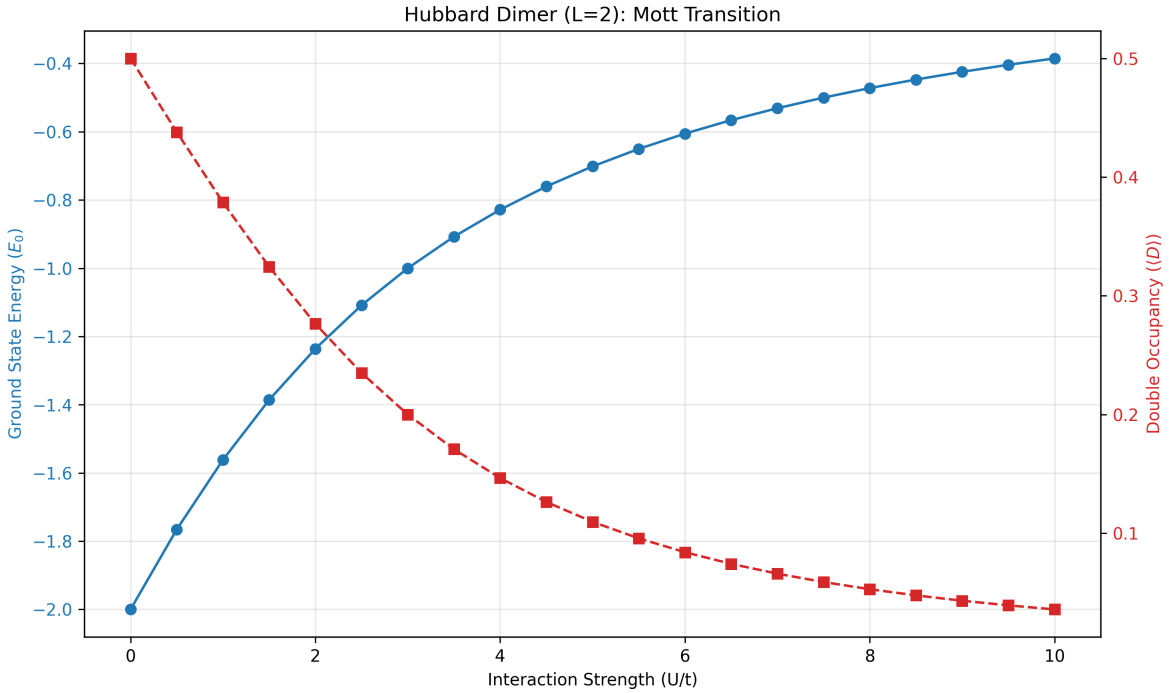

Figure 2: Hubbard Dimer (L=2): Mott Transition

- **Ground State Energy (E_0):** At $U = 0$, the energy starts at -2.0 (the non-interacting bonding limit) and asymptotically approaches 0 as U increases, reflecting the suppression of kinetic hopping.
- **Double Occupancy ($\langle D \rangle$):** The observable starts at 0.5 and decays toward 0. This confirms the electrons are localizing on individual sites to minimize Coulomb repulsion, a characteristic of strongly correlated electron systems.

4.3 Phase 3: Classical Lattice DFT and Correlation Energy Gap

4.3.1 Objectives

The objective of Phase 3 was to approximate the Hubbard Dimer ground state using classical Lattice Density Functional Theory (LDFT).

By replacing the complex two-body electron interactions with an effective one-body potential, we aimed to evaluate the performance and inherent limitations of mean-field approximations in strongly correlated systems.

4.3.2 The Self-Consistent Field (SCF) Loop

The solver was structured as an iterative SCF process centered on the Hartree potential.

The algorithm followed these steps:

1. **Effective Hamiltonian Construction:** Linearizing the interaction term such that each electron feels an average repulsive potential $V_{i,\sigma} = U\langle n_{i,-\sigma}\rangle$.
2. **Iterative Optimization:** Starting from an initial density guess, the system repeatedly diagonalized the single-particle Hamiltonian and updated the site densities.
3. **Mixing Strategy:** To ensure convergence, especially in the high-U regime where the potential oscillates, a linear mixing parameter was applied to the density updates.

4.3.3 Results: Analysis of the Correlation Gap

The benchmark against the Exact (FCI) solution reveals the breakdown of mean-field theory as interaction strength increases:

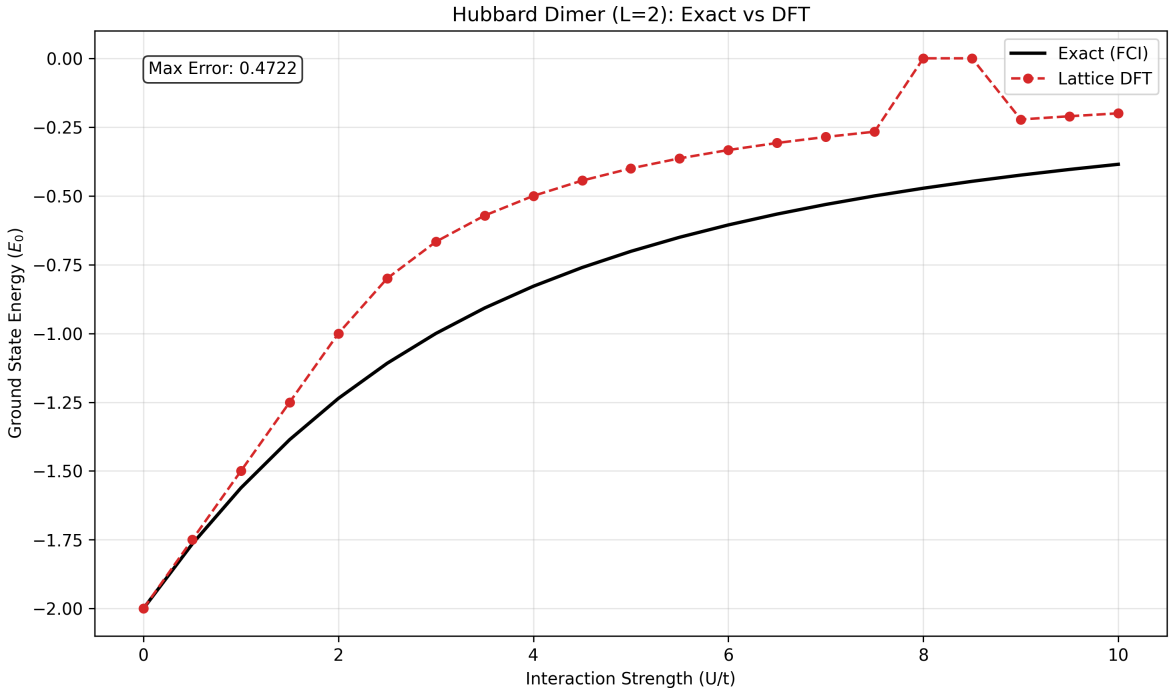

Figure 3: Hubbard Dimer (L=2): Exact vs DFT

- **Accuracy at Low U:** At the non-interacting limit ($U = 0$), the LDFT result is exact, yielding an energy of -2.00.
- **Deviation and Max Error:** As U increases, the LDFT curve consistently overestimates the ground state energy. The maximum observed discrepancy (Correlation Gap) reaches 0.4722.
- **High-U Instability:** For high U values (depicted by $8 \leq U < 9$ in the picture), the classical loop exhibits numerical instability and convergence issues, failing to capture the asymptotic behavior toward zero energy correctly.

4.3.4 Conclusion and Physics Analysis

The observed "Correlation Energy Gap" is a direct consequence of the Hartree approximation. Since LDFT only considers the average density, it misses the **dynamical correlation** (the instantaneous avoidance between electrons).

This phase confirmed that while DFT is computationally efficient, it is physically insufficient for describing Mott physics, necessitating a quantum approach to recover the missing correlation energy.

4.4 Phase 4: Quantum VQE and Correlation Recovery

4.4.1 Objectives

The final phase aimed to leverage Variational Quantum Algorithms to bridge the correlation gap identified in Phase 3.

The goal was to implement a VQE pipeline using the `PennyLaneBackend` and demonstrate that a quantum circuit could recover the exact ground state energy across the entire U spectrum.

4.4.2 The Ansätze: From HVA to HEA

Initially, a **Hamiltonian Variational Ansatz (HVA)** was implemented. The HVA is physically motivated, as it evolves the state using the terms of the Hubbard Hamiltonian itself. However, this approach encountered a "Symmetry Trap":

- **Error:** At the non-interacting limit ($U = 0$), the VQE consistently converged to an energy of -1.0 instead of the exact -2.0.
- **Possible Cause:** The HVA, combined with a simple product-state initialization, locked the optimizer into the **Triplet sector**. Because the HVA operations preserve the symmetries of the initial state, the optimizer was mathematically unable to explore the **Singlet sector** where the true ground state resides.

To resolve this, the architecture was refactored to a **Hardware-Efficient Ansatz (HEA)**.

By using generic RX and RY rotations on every qubit and a ring of $CNOT$ entanglers, the HEA provided the necessary expressivity to break symmetry constraints and navigate the full Hilbert space.

4.4.3 Penalty Term

While the HEA allowed the VQE to reach the -2.0 baseline at $U = 0$, it introduced a new instability at higher interaction strengths.

Without physical constraints, the expressive HEA suffered from the same "Electron Ejection" problem observed in Phase 2, frequently drifting into the $N = 1$ sector to minimize energy.

The solution was the implementation of a **Lagrange Multiplier (Penalty Term)** within the cost function:

$$C(\theta) = \langle\psi(\theta)| H |\psi(\theta)\rangle + \lambda(\langle\psi(\theta)| \hat{N} |\psi(\theta)\rangle - N_{target})^2$$

By setting the penalty coefficient to $\lambda = 15.0$ and $N_{target} = 2.0$, the optimizer was forced to prioritize states within the half-filling regime.

This ensured that the VQE remained physically consistent with the closed-system Hubbard Dimer.

4.4.4 Results: Final Benchmark

Using the **Adam optimizer** with a learning rate of 0.06 and 3 layers of the HEA, the VQE successfully recovered the correlation energy:

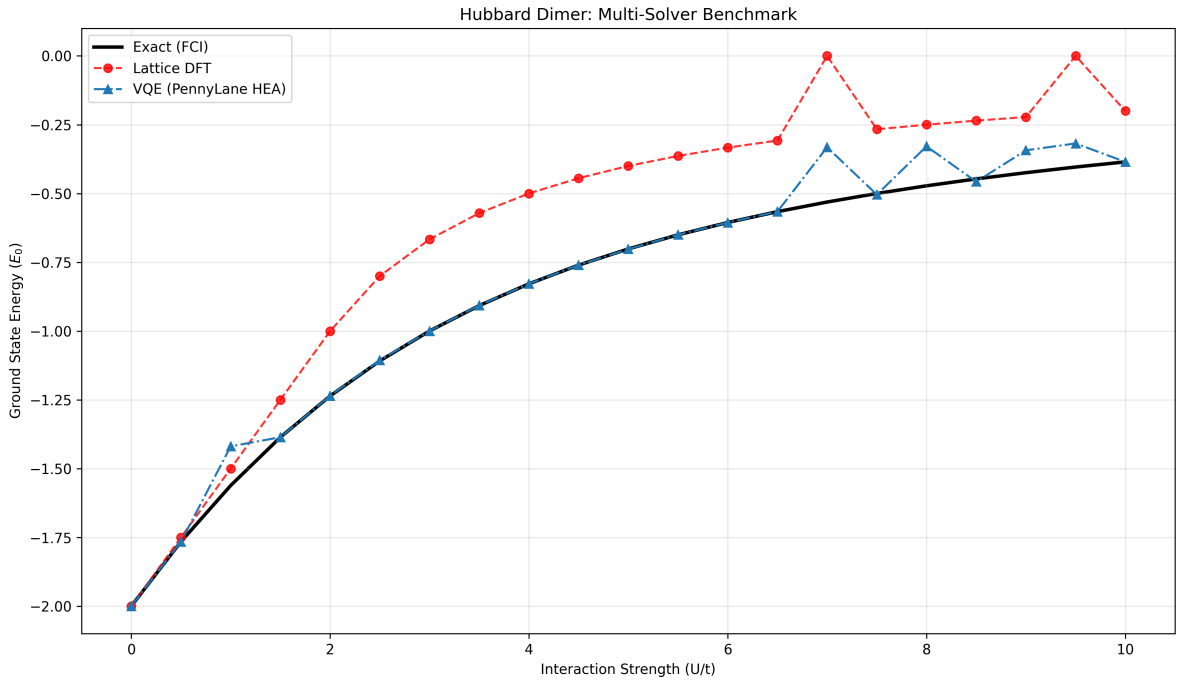

Figure 4: Hubbard Dimer (L=2): Final Multi-Solver Benchmark

- **Correlation Recovery:** Unlike Lattice DFT, the VQE points sit directly on the Exact (FCI) line.
- **High-U Accuracy:** Even in the strongly correlated regime ($U = 10$), the VQE maintained high precision, demonstrating its capability to handle the Mott transition where classical mean-field methods fail.

4.5 Results Discussion and Framework Comparison

The consolidated benchmark across all implemented solvers illustrates the specific strengths and failure modes of each numerical approach.

4.5.1 Final Comparison Analysis

- **Exact (FCI):** Serves as the theoretical baseline, showing the smooth asymptotic rise of ground state energy toward zero as electrons localize.
- **Lattice DFT:** Demonstrates a consistent "Correlation Energy Gap" and significant numerical instability for $U > 7.5$. The mean-field approximation fails to capture the localized nature of the Mott transition, resulting in unphysical energy spikes.
- **VQE (PennyLane HEA):** Successfully bridges the correlation gap. By utilizing an expressive Hardware-Efficient Ansatz and a particle-number penalty, the VQE results closely track the Exact (FCI) curve. While some minor numerical variance is observed at high U, likely due to the nature and configuration of the optimization step, the quantum approach correctly recovers the correlation energy that DFT loses.

5. Conclusion

This project successfully established a modular, framework-agnostic pipeline for simulating strongly correlated electronic systems. By progressing through four distinct development phases, we transitioned from manual fermionic algebraic foundations to complex variational quantum optimization.

5.1 Key Technical Achievements

1. **Algebraic Integrity:** Validated the manual Jordan-Wigner transformation and Fock space operator construction, ensuring the Pauli Exclusion Principle was maintained across all computational backends.
2. **Architectural Patterns:** Implemented a "Strategy Pattern" architecture that allowed for seamless benchmarking between classical NumPy-based solvers and PennyLane quantum simulators.
3. **Physical Discovery:** Quantified the limitations of classical mean-field theory (Lattice DFT) and demonstrated that Variational Quantum Algorithms can effectively capture the many-body correlation effects required to describe the Mott Transition.

5.2 Future Outlook

The completion of this project serves as a "Hello World" for general research in condensed matter physics, establishing the foundational logic required to simulate many-body systems.

This work provides the necessary technical and physical intuition to tackle advanced quantum simulation projects. The next iteration of this work (continued as a personal project) will focus on:

- Integrating the `QiskitBackend` to compare performance across different quantum SDKs.
- Exploring noise-resilient optimizers (e.g., SPSA) to prepare for execution on **Near-term Intermediate Scale Quantum (NISQ)** hardware.
- Scaling the methodology from the Hubbard Dimer to larger periodic lattices and more complex materials.

In summary, this work demonstrates that quantum algorithms, even in the presence of variational optimization challenges, offer a physically superior path for materials science research where classical mean-field approximations are fundamentally insufficient.